

3D printed pyrography: Using wood filament and dynamic control of nozzle temperature for embedding shades of color in objects

Kongpyung (Justin) Moon^a, Jaeseong Yi^a, Valkyrie Savage^b, Andrea Bianchi^{a,*}

^a Department of Industrial Design, KAIST, Daejeon, Republic of Korea

^b Department of Computer Science, University of Copenhagen, Copenhagen, Denmark

ARTICLE INFO

Keywords:

3D printing
3D pyrography
Wood filament
Rapid prototyping

ABSTRACT

Colors enhance the esthetic and functional aspects of three-dimensional (3D) printed objects via material extrusion (MEX). However, existing 3D printing techniques require additional materials and hardware that are either challenging to calibrate or too costly for average 3D printing users. This paper presents a fabrication technique we call 3D printed pyrography, which enables printing multiple shades of color and gradients using a wood filament and a single-nozzle extruder. We investigate the effects of printing temperature and speed on the color properties of wood filament (ColorFabb). Using Euclidean distance in CIELAB color space, we employed perceptual metrics to quantify color differences between samples with different print temperatures (minimum: 195°C, maximum: 300°C, and 5°C increment). As a result, we identified all samples had perceivable discrete colors ($\Delta E \geq 1$), and, by applying a more conservative threshold, we can refine the count to sixteen distinct colors ($\Delta E \geq 2.3$). This approach underscores the sensitivity of color perception to printing parameters and highlights the utility of ΔE in CIELAB parameters in discerning color differences in 3D printed objects. Furthermore, we encapsulate this information in a custom software interface. This tool allows users to specify shades or map photographic images directly onto 3D surfaces, and generates the G-code that modulates the nozzle temperature and achieves the desired shading. We demonstrate 3D printed pyrography through 11 applications, such as enhancing visual esthetics, offering visual guidance, and embedding markers to merge digital information with physical objects.

1. Introduction

3D printing with multiple colors opens many opportunities for visual expression and rich applications not possible with monochromatic objects. For example, previous works used colors to enhance the esthetics of 3D artifacts with photographic images, logos, and labels placed onto their surfaces [53], or to convey structural properties of geometry by showing FEM simulation results as colors in the 3D printed object itself [36]. Even binary black and white colors, despite their limited expressiveness, are sufficient to create AR markers [14] or display visual operating instructions, e.g., on a 3D printed kettlebell [64].

Motivated by these scenarios, researchers have tried to find methods to embed colors directly in 3D printed objects, specifically with Fused Filament Fabrication (FFF) machines—one of the most common type of 3D printers. Currently, 3D printing in colors can be achieved by printing a filament composed of multiple colors [55], by using multiple independent extrusion nozzles (one per filament) [16,18,48], by cutting and

reconnecting filaments which are later fed through a single extruder [43], or by adding colored ink to filament on-demand from a CMYK cartridge [47] or marker pens [38,50]. While these techniques provide wide color options, they often require multiple filaments or specialized hardware that is not commonly available to the average user, and require expertise and delicate calibration processes. This paper introduces *3D printed pyrography*, a novel technique and software system that allows users to 3D print artifacts with multiple and distinct shades from a single color, using a wood-based filament extruded from a single-nozzle FFF printer. Our approach does not require manual intervention (e.g., changing filaments) or hardware upgrades. Instead, it appropriates the pyrography technique [25,46] of charring wood to alter its color appearance, and applies it to 3D printing by generating G-code that dynamically controls the temperature of the nozzle (and thereby the wood particles in the filament) during the printing process. Through a rigorous material investigation of how wood filament is affected by nozzle temperature and extrusion speed, we were able to

* Corresponding author.

E-mail address: andrea@kaist.ac.kr (A. Bianchi).

identify 16 distinct, achievable color shades. With this knowledge, we developed an automatic software pipeline and a 3D slicer that let users selectively apply different color shades to various parts of 3D printed artifacts that—despite being printed using the same material and a single-nozzle machine—look unique and different from each other. For example, Fig. 8 shows the same 3D character printed with different shading patterns, including discrete color patches and gradients, to achieve completely distinct looks despite being printed with the same material. In some cases, these shades provides functional and meaningful information that would be lost if printed in a single color: the horizontal markings on the cone in Fig. 8b are essential to signify that this is a safety cone and not a generic indicator. The list of other possible example usages goes on and includes placing text and logos on 3D objects (Fig. 10a), texture-mapping surfaces with images (Fig. 7d-e), embedding AR markers (Fig. 11a), and using color shades as visual guidance during the assembly of parts (Fig. 10b-c).

The contributions of this paper are threefold:

- A rigorous exploration of how wood-based filament is affected by nozzle temperature and extrusion speed. An investigation to identify the distinguishable color variations in printed wood filament, a study that could be extended to other printed wood materials. The number of colors and the printing parameters supported by our system.
- A custom tool, implemented as a Rhino plugin, that allows users to apply discrete or gradient shades on parts of a geometry. Based on the user input, the software generates G-code instructions to dynamically control the nozzle temperature which results in charring the wood filament during printing.
- A set of diverse applications that describes the design space afforded by selectively applying shades of colors to the surface of a 3D model. Inspired by previous work [36,55] we present applications that enhance the esthetics of the 3D artifacts (e.g., color patches, gradients, texture mapping) but also highlight usages for functional prototypes (e.g., visual markers and visual guidance).

2. Material and methods

2.1. 3D printed pyrography

This paper presents a novel method to generate multiple shades of color with a single wood filament using a single-extruder FFF printer without hardware upgrades or additional fabrication steps. We achieve this by selectively *charring* (or *toasting*) the wood fibers of an off-the-shelf wood filament while printing—a technique known as pyrography [46]. The principle of this technique is the same as that used when engraving with a laser cutter [29], or manually burning wood with a soldering iron for arts and crafts [46]. We perform our tests using the *ColorFabb* wood filament [10], which is composed of 70% of PLA and 30% of recycled pinewood fibers.

2.2. Wood filament investigation

The process of charring is affected by two distinct parameters: the **temperature** of the nozzle, and the **extrusion speed** at which the filament travels through the nozzle (i.e., the duration for which a filament is heated). The following section investigates the effect of these two parameters on material color through two separate studies; we aim to determine the maximum number of perceivably distinct colors that can be printed and the most reliable way to produce consistent results.

2.3. Relating temperature and color for wood filament

The first study investigates the effect of nozzle temperature on

material color. For this and all following studies, a 3D printer¹ running Rep-Rap firmware equipped with a direct-drive extrusion E3D volcanic nozzle (0.8 mm diameter) was used. A 1.5× extrusion multiplier was applied to prevent clogging.

To test the relationship between temperature and color we printed twenty-two cuboid samples (10 × 10 × 10mm [63]) with temperatures from 195°C to 300°C at intervals of 5°C, while maintaining a 100 mm/min extrusion speed. This range was chosen by following the manufacturer's recommended printing temperature (195°C to 220°C) and extending it to 300°C, which is the maximum temperature that our nozzle can achieve. The 5°C increment is based on the fact that our printer's internal firmware starts printing within ±2.5°C of a programmed temperature [15], i.e. the smallest reliable step size.

The printed samples were then photographed in a dark room environment with a fixed light source and camera setting (Canon EOS 6D, 1/800, ISO 4000, F14). To ensure consistency across the photos, a fixed white balance of 5500 K was applied to all photos. One representative RGB value was sampled from each photo by applying an averaging filter on the top surface of each cuboid, where layer lines would not introduce shadows. As in [62], these values were then plotted onto a CIELAB color space graph (International Commission on Illumination²) with a custom Python script using an *OpenCV*³ package for converting RGB to CIELAB through a standard CIE scale (L^* : 0–100, a^* and b^* : centered 0). The total number of perceivably-distinct colors was defined by computing the Euclidean distance (ΔE) between the samples in the CIELAB space, where $\Delta E = 1$ is a just-noticeable color difference (JND) [39]. We openly share the python-script used in this method in a Github repository.⁴

2.3.1. Results and findings from temperature and color

As shown in Fig. 1 and Figure A.1 of the Appendix, the pairwise distance between all the samples is greater than the CIE standard for color difference ($\Delta E = 1$), with an average of 2.6 ΔE (SD = 1.04, min: 1, max: 4.75). This finding reveals that all 22 shades of colors printed at different temperatures are visually distinguishable from each other because they are above the just-noticeable-difference (JND) threshold of $\Delta E = 1$. Furthermore, the finding demonstrates that a 5°C difference in nozzle temperature is indeed sufficient for our purpose to create distinguishable colors.

However, prior works also suggest that the CIE standard ($\Delta E = 1$) is an optimistic theoretical value, which means that not all users may be able to easily discern these colors. Thus, they proposed a more conservative JND with a ΔE of 2.3 [1,39]. Following this suggestion, we extracted from our original samples a subset with a JND threshold of $\Delta E = 2.3$ between consecutive values. For example, Fig. 2 shows a difference of $\Delta E = 2.56$ between the sample printed at 210°C vs. its immediate predecessor (printed at 205°C). However, the sample printed at 225°C was not sufficiently distinguishable ($\Delta E \leq 2.3$) from its immediate predecessors (220°C and 215°C), but yet very different from the sample printed at 210°C ($\Delta E = 3.1$). Following this approach we were able to identify 16 distinguishable shades of color—the 15 shown in Fig. 2 plus the initial reference value of the cuboid printed at 195°C. The average Euclidean distance between adjacent pairs of these sixteen samples is $\Delta E = 3.5$ (SD: 1.05, min: 2.35, max: 5.67).

From these results combined we can conclude the following: firstly, by altering the nozzle temperature in steps of 5°C we were able to print 22 distinguishable shades of color ($\Delta E \geq 1$). Following a more conservative JND of $\Delta E = 2.3$,

we were still able to identify 16 unique shades spanning a total Euclidean distance of $\Delta E = 44.82$. Secondly, while 5°C intervals were sufficient to uniquely identify shades for the first case, in the second case

¹ <https://e3d-online.com/>

² CIE 15:2004

³ <https://opencv.org/>

⁴ <https://github.com/makelab-kaist/3DPyrography>

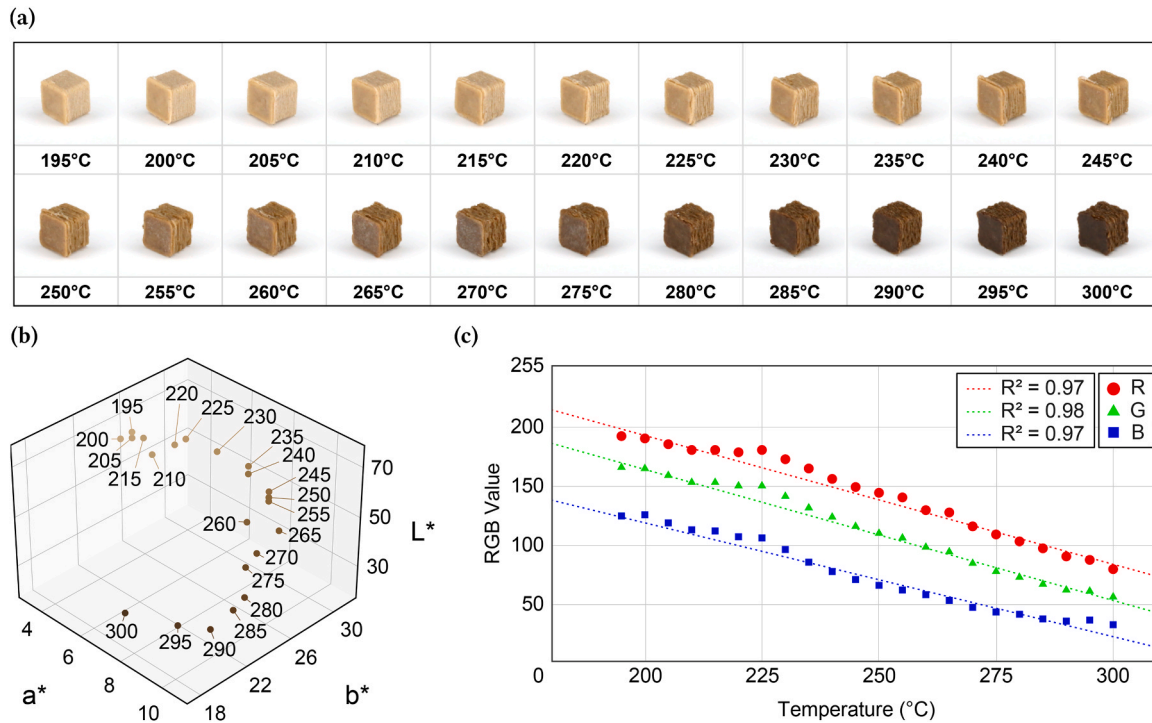


Fig. 1. a) Table of cuboid samples organized by printing temperature. b) CIELAB plot of RGB values extracted from cuboid samples. c) Relationship between printing temperature and RGB values.

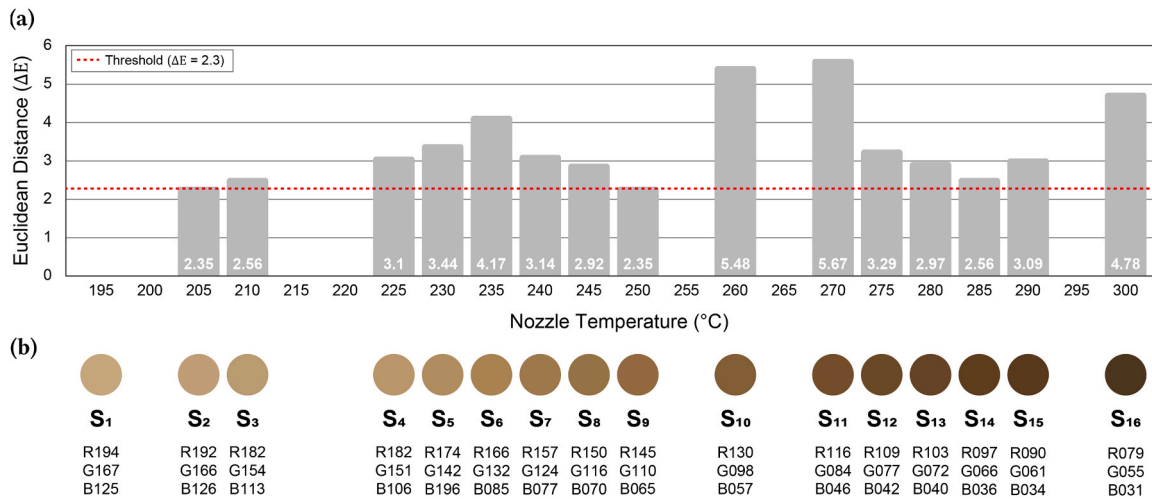


Fig. 2. a) The sixteen distinct temperature-driven shades with an Euclidean distance greater than 2.3 between consecutive temperature samples, and b) their color swatches with RGB values.

shades were printed at different discrete intervals, up to 20°C. It is also worth noting that the RGB graphs shows a linear relationship between colors and temperatures ($R^2 \geq 0.97$). Finally, greater distinction at the expense of fewer colors can be achieved by further doubling the ΔE , which would result in colors that are even more distinguishable. This threshold is user-dependent or application-specific, and can be explored by using our methodology, above.

2.4. Extrusion speed-color relationship for wood filament

The second study investigates the effect of extrusion speed on material color. A total of fifteen cuboid samples were printed with three different nozzle temperatures (195, 250, and 300°C) and five different speeds, doubling at each step in the range of 100–1600 mm/min. The

printed samples were photographed and plotted as in the first study. The speed of 100 mm/min was the same as used in the previous experiment and serves as a baseline condition.

2.4.1. Results and findings from speed and color

Fig. 3 shows that the average Euclidean distances (ΔE) between the two most extreme shades of color in a set are 9.97, 24.42, and 47.72 at respectively 195°C, 250°C, and 300°C. Furthermore, we observe that, for a given temperature, increasing the speed results in lighter shades, while decreasing it results in darker ones—the role of speed is merely that of modulating the amount of charring by changing how long the filament is exposed to the nozzle heat. Finally, we observe that the relationship between speed and color is non-linear: fitting logarithmic curves gives $R^2 \geq 0.97$ in all cases (Fig. 3b).

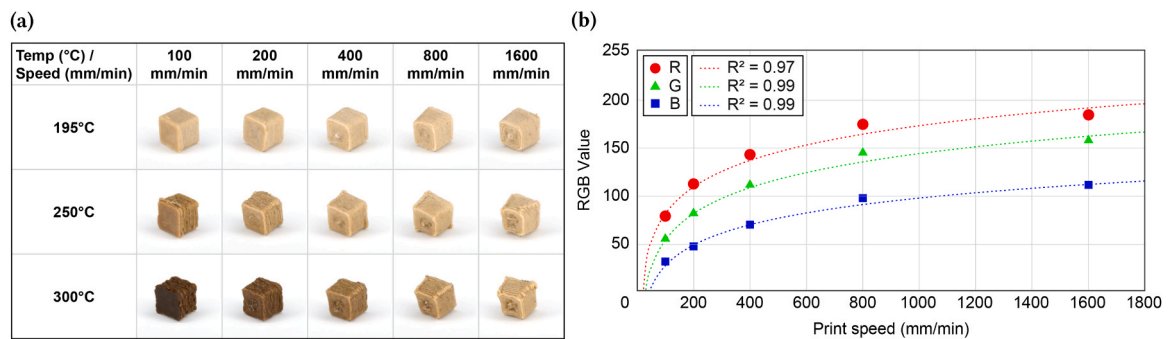


Fig. 3. a) Table of cuboid samples organized by printing temperature and extrusion speed. b) Relationship between speed and RGB values at 300°C.

2.5. Discussion on results and findings

The combined results of these studies tell a simple story. Both nozzle temperature and extrusion speed affect the range and number of color shades that can be printed using the *ColorFabb* wood filament [10]. Temperature and colors have a linear relationship (R^2 never below than 0.97), and, if we select a ΔE of 2.3, we can uniquely identify 16 colors. Extrusion speed also results in changes in colors, however, these changes are more difficult to control. Therefore, for this paper, we decided to use temperature-control alone as a method to generate shades for their simplicity and reliability. For the rest of the paper we identify the 16 unique shades of colors by their print temperature or by name (e.g., S_{16}).

3. Theory

This paper is closely related to previous literature on hardware and software based multi-color 3D printing techniques, and previous functional exploration of wood-impregnated 3D printed material.

3.1. Multi-color FFF printing

FFF printers work by depositing molten thermoplastic filament layer-by-layer from a heated nozzle, constructing stacked 2D paths that eventually form three-dimensional objects. Although it is certainly possible to add colors to monochromatic 3D printed artifacts using post-printing methods (e.g., spray-painting [19], acrylic-painting [27], or hydro-dipping [65]), researchers have pursued methods for creating colorful objects directly through the printing process, for example, by using filaments of different colors and multi-nozzle FFF printers [16,48]. This approach is straightforward but requires less common, more expensive printers, which also require careful calibration for various nozzles to ensure filament alignment.

Filament switching machines [43,48] *cut and re-connect* multiple filaments into one before feeding it through the nozzle, but also require additional hardware and are prone to jamming at filament fuse points. Programmable Filament [55] creates a multi-colored filament by printing multiple color filaments into a single strand, which is later used to print a colored object. While this technique does not require additional printer hardware (as the *cut and re-connect* approach does) and allows for arbitrary numbers of colors, it involves the additional step of printing a programmed spool from individual color filaments, which adds to printing time and labor.

A simpler alternative to using multiple color filaments is to ink them just before printing. This technique involves coloring white or transparent filaments with a marker, eliminating the need for switching between filaments. *3DPrint-Colorizer* [50] colors the outer surface of a printed object layer by layer with a permanent marker that is attached to the 3D printer's tool head, while *Automated Filament Inking* [38] colors the filament before extruding it through a heated nozzle. Both methods require additional hardware and meticulous calibration since even

minor deviations can compound throughout the print, resulting in colors appearing incorrectly in the final object.

Finally, there are commercially-available machines such as *da Vinci Color* [47] that use CMYK ink cartridges to color prints made from PLA filament specially designed to absorb ink, but the ink is prone to drying due to its constant exposure to heat inside the machine [38,47]. Overall, inking offers the ability to print a wide range of colors with a single material, but this benefit is offset by the need for hardware upgrades, color markers or ink cartridges, and a careful calibration process. Figs. 4 and 5

3.2. Thermally-activated filaments

Heat is one of the possible parameters that can be used to dynamically morph the shape [2,42,54,60,61] of 3D printed objects, or temporarily shift their color hue via thermochromic pigments [34].

Heat-based shape-changing leverages the residual stress accumulated during the initial printing process [44]. Polymer chains that have been stretched and cooled release this residual stress upon being reheated beyond the glass transition temperature, leading to a contraction along the printing direction [44]. Several researchers have applied this effect on both single- [54,60,61] and multi-material [2,42] prints to create large-scale objects such as shape-changing furniture [61], support-free printing [2], collision-free morphing actuators [42], and perfect-fit medical casts [54].

Heat has also been used to temporarily modify the colors of a completed printed artifact. Thermochromic filament changes color when subjected to temperatures above its color-activation threshold (e.g., 32°C [7]) and reverts to its original color upon cooling below the threshold. This repeatable process allows designers and researchers to 3D print objects that can shift between two colors. For example, thermochromic material is used in a variety of applications including wearable bracelets that can monitor fever [13], displays that visualize the charge of a battery [20], and level-sensors for containers of liquids [23]. *ChromoFilament* [34] is also based on thermochromic pigment mixed with thermoplastic, but it focuses on color as a proxy for when a heated plastic object is safe to be touched and modified by hand.

All these projects use heat *after printing* to activate fabricated objects (i.e., mechanical motion or temporary visual changes). In contrast to these, our approach focuses on heating *during printing* to achieve a *permanent* change of the look 3D printed artifacts through color shades.

3.3. 3D Printing wood filament

Wood, a naturally abundant renewable organic material that comes from plants, can be combined with various 3D printing materials such as polymers [10], gypsum [24], bio-polymers [35], and nanocomposites [5]. Commercially-available wood filaments for FFF printers use Poly-Lactic Acid (PLA) as a binder for fine wood particles, enabling it to be used for 3D printing objects with a wood-like look and feel [10]. Prior works that used wood filaments have studied the mechanical [4,17,21,

System / Attribute	Multiple Extruder Machine [12,35]	CMYK inking [34]	Filament Switcher [30]	3D Print Colorizer [37]	Filament Inking [27]	Programmable Filaments [40]	3D Printed Pyrography
Single Extruder	×	✓	✓	✓	✓	✓	✓
Single Input Material	×	×	×	×	×	×	✓
Single Step Printing	✓	✓	✓	✓	✓	×	✓
No Additional Hardware	×	✓	×	×	×	✓	✓
Low-Cost	×	×	×	✓	✓	✓	✓
No Calibration	×	✓	×	×	×	×	✓

Fig. 4. Comparison table of related work.

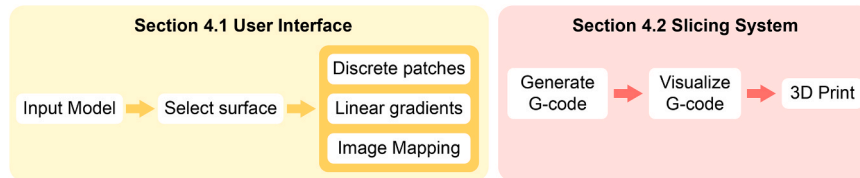


Fig. 5. Software system overview.

33,56] and thermal properties [9,37,56] of 3D printed wood. Higher wood content inside the filament could increase the modulus tensile strength (GPa) but decreases the tensile strength (MPa) [12,33]. The poor bindings between wood content and PLA fails to encapsulate wood particles, leading to poor bonding and load transfer [33].

The color of the wood filament also depends on both the type and amount of wood particles. Studies have explored various wood types in 3D printing materials, such as beech [32], aspen [56], poplar [4], and pine [21,45]. For instance, filaments with spruce tree particles [45] have a lighter color than the ones with beech or poplar [4,32] due to the natural color of the source material. The color can also be altered by increasing or decreasing the concentration of wood particles in the filament, with higher wood content resulting in darker colors [12]. While both variables may influence the coloration of the filament, the process of fabricating filaments from raw materials is not readily accessible to the average 3D printer user. This additional fabrication step also imposes an elevated labor requirement preceding the printing phase. Furthermore, these filaments would still only be capable of printing a single color without the techniques mentioned in the previous sections (i.e., changing or blending filaments, or inking).

These limitations reveal an opportunity for a more user-friendly approach to *selectively* customize the color of wood filament.

4. Results

This section describes our software editor developed to support 3D printed pyrography. Using this tool, the users can import a digital geometry and selectively apply various colors to portions of its surfaces using three shading styles: discrete patches, linear gradients of four directions, and image mapping. The results of this input can be immediately visualized directly in the software, and when the user is ready, the system generates the G-code instructions that are used for 3D printing. The process results in printed artifacts made with wood filament and shaded (i.e., charred) as specified by the user using the software interface.

The graphical user interface and the custom slicer were developed in C# with Rhinocommon API⁵ and Human UI,⁶ a Rhino Grasshopper add-on.

4.1. User interface: input and real-time visualization

We developed an open-sourced software interface⁷ as an extension plugin for Rhino 3D that allows users to apply various color shades to 3D models and to digitally visualize the results. Users first import geometry in any 3D file format (e.g., .stl, .obj, .3 dm). By clicking on the polygons of interest and buttons on the user interface we provided (Fig. 6a), the users can then choose among three types of shading methods: discrete patches, linear gradients, and image mapping.

4.1.1. Discrete patches and linear gradients

For discrete and gradient shadings, users select a color from the interface (Fig. 6a) and assign it to the polygon mesh of a 3D geometry. The interface provides, via visual buttons, options for 16 discrete shades (determined through the material investigation) and linear gradients in four directions. The gradients are linear interpolations of two arbitrary colors (e.g. from S_1 to S_{16} with the minimum temperature increment of 5°C) along the vertical or horizontal axis (left-right, right-left, top-down, bottom-up) and span the whole user selection. During this process, the software provides a real-time visualization of the assigned shades (Fig. 6b).

4.1.2. Image mapping

To create an image-driven 3D pyrography, the end user uploads an image file (e.g., .jpg or .png) of arbitrary size, and selects the target surface. This surface can be either flat, as in Fig. 7b, or curved, as in Fig. 7c. The color at each point of the 3D surface is computed by extracting the greyscale value of the corresponding pixel in the image, and interpolating it across the full range of color shades.

4.2. Slicing and printing

Once the user has finalized the shading of the 3D digital model in the software, the system proceeds with creating a G-code file using our custom slicer. The slicer produces the machine instructions for the path and temperature control used by the printer, and a visualization of the printing paths within the editor that enables users to quickly inspect whether the shades they have applied to the 3D model correspond to the desired final effect (Fig. 6d).

4.2.1. Generating G-code

Our custom slicer follows similar procedures to conventional FFF

⁵ <https://developer.rhino3d.com/api/rhinocommon/?version=8.x>

⁶ <https://www.food4rhino.com/en/app/human-ui>

⁷ <https://github.com/makelab-kaist/3DPyrography>

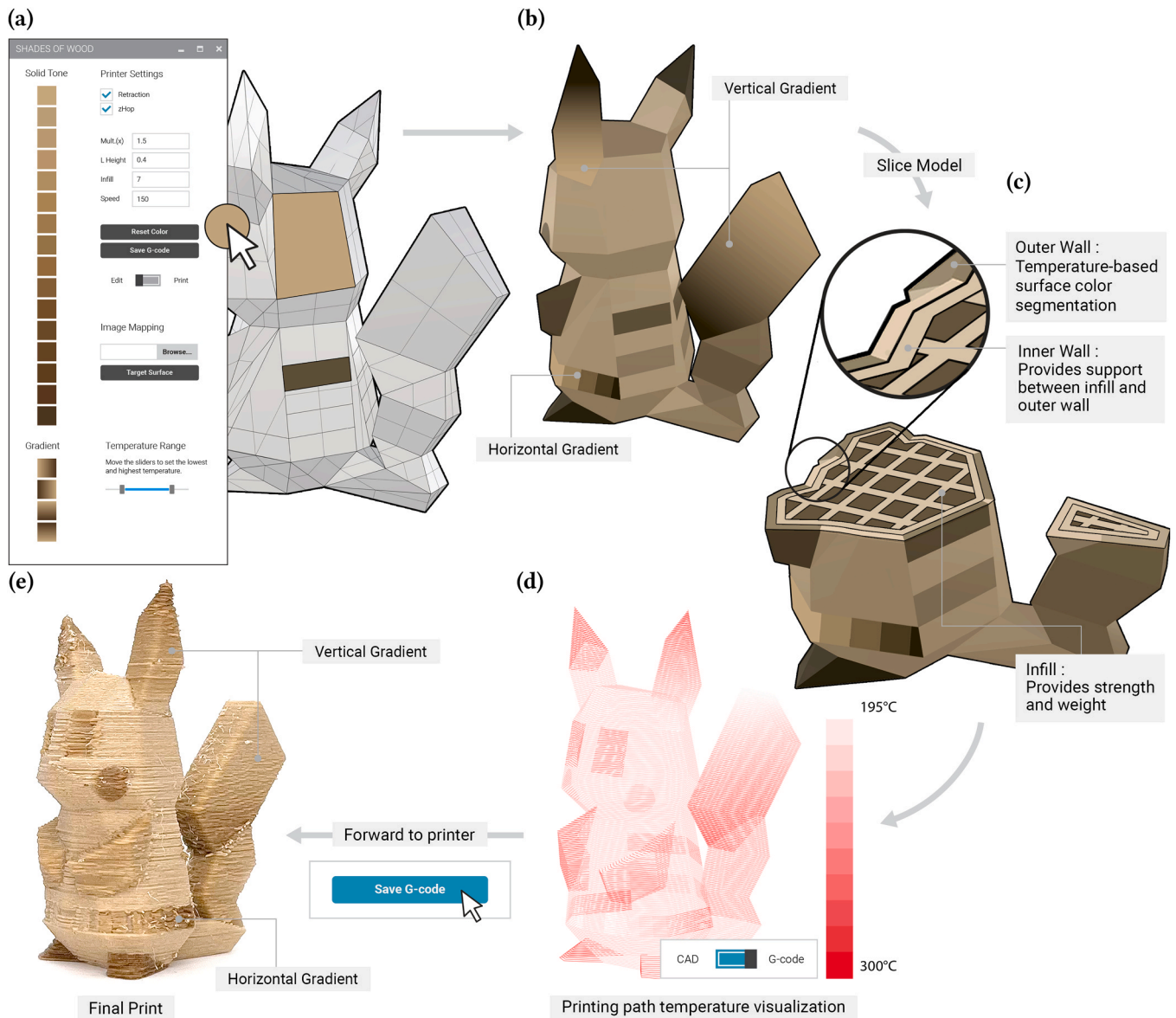


Fig. 6. a) Selecting and assigning shades on a geometry. b) Real-time visualization of the assigned shades. c) Cross-section view revealing the three types of printing paths: outer walls, inner walls, and infill. d) Visualization of the final printing paths and of the corresponding temperatures. e) Final result.

slicers [11,49,52]. It creates an extrusion trajectory—known as the printing path—layer by layer (here, 0.4 mm layer height), then clusters printing paths (i.e., outer walls, inner walls, or infill) and sorts them in the correct printing order: inner walls → infills → outer walls. However, unlike conventional slicers, our software is capable of injecting changes in nozzle temperature at specific printing path coordinates. Specifically, the software alters the temperature settings for each printing path of the outer wall by issuing a G-code command before moving the nozzle to the desired location and extruding the filament.

The algorithm operates by generating G-code instructions for the individual layers of a geometric model. Each layer represents a horizontal cross-section of the initial model, wherein the outer boundary forms the shell, and the interior is filled with a grid-like structure called infill (Fig. 6c). The infill serves as structural support and is printed at a speed of 1600 mm/min and a temperature of 195°C, as recommended by the filament manufacturer. The shell, which can be further categorized into inner and outer walls, plays a crucial role in defining surface details and shading. Specifically, the inner wall is printed at a thickness of 1.2 mm (also at 195°C) and is subsequently outlined by another 1.2 mm print line, the outer wall. Temperature control is selectively

applied to the outer wall to achieve desired shading effects. We printed the inner structures (e.g inner wall and infills) with the nozzle temperature of 195°C regardless of the outer wall's color shade in order to minimize the structural damage caused by thermal degradation of outer wall.

The shading process for the outer wall functions as follows: for each layer, the system calculates the perimeter of the model's cross-section and extracts a poly-line. The poly-line is divided by the points where polygons with different user-assigned shades intersect. This results in series of poly-line segments with different color-shades. Finally, the system generates G-code instructions to both heat the nozzle to the necessary temperature for an assigned color and extrude the filament along the specified paths. To minimize the number of times the nozzle temperature needs to be adjusted, all paths are sorted by temperature in ascending order.

4.2.2. G-code visualization

The system provides a G-code visualization directly in the user interface. This is useful to verify how color shades are applied to the sliced 3D geometry, approximating the look of the printed artifact. Each

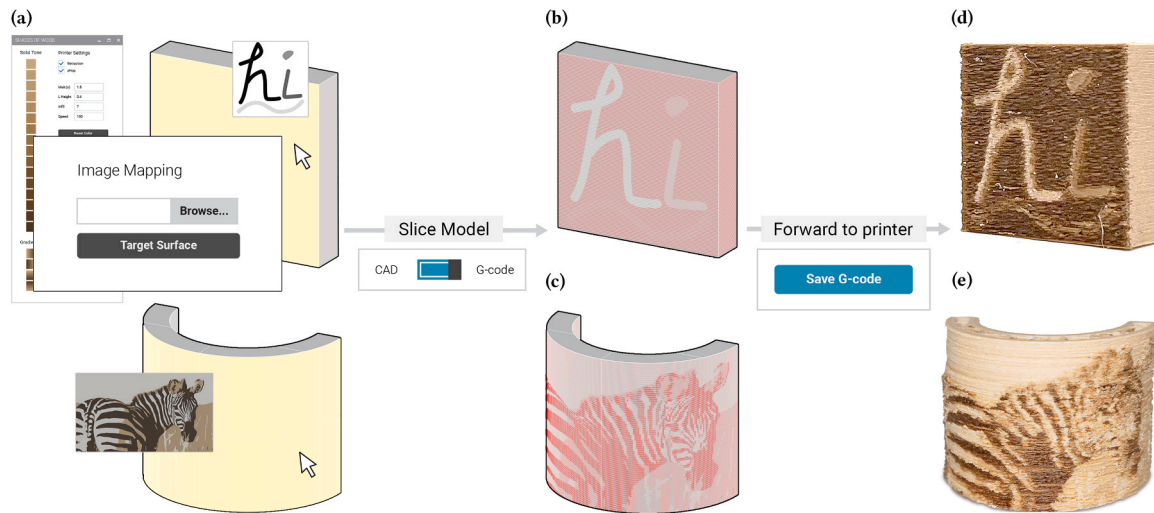


Fig. 7. a) Mapping an image to a flat and curved target surface. b), c) Visualization of the final printing paths and the corresponding temperatures. d), e) Final result.

printing path is color-coded in a gradient from white (195°C) to red (300°C), representing the temperature at each point of the path. This allows users to confirm the segmentation of the printing path, the number of layers in the overall geometry, the amount of infill, and the printing temperature created by the custom slicer.

4.2.3. 3D printing

Our software interface allows saving the G-code in a file compatible with the RepRap firmware⁸, allowing direct export to a single-nozzle FFF printer. The printer interprets the sequence of G-code commands to guide the nozzle movements in the X, Y, and Z coordinates and applies temperature changes for each path using the built-in temperature command. For each temperature adjustment, the machine pauses and waits until it reaches the target temperature (e.g., 195°C, 230°C, or 300°C) and then continues with the printing. In our configuration, temperature is not changed while extruding or moving the nozzle to prevent clogs (refer to limitations section).

4.2.4. Adjusting temperature during printing process

To adjust the nozzle temperature we used the following method. The extruder moves outside the printing bed using the G1 command. To change the temperature, we issue the RepRap standard M109 *Set Extruder Temperature and Wait* command with the R *Accurate Target Temperature* parameter to set the target temperature and wait until the nozzle reaches the set temperature. Cooling fans are enabled using the M106 S255 command only when the target temperature is below the current one. To accelerate the heating time and prevent nozzle clogging, the fan is kept off while raising the temperature and during the printing process. We measured the heating and cooling duration of the extruder nozzle for temperature changes of 10°C and of 100°C, finding that cooling is faster than heating. All measurements are averaged from three samples, results are reported in Table 1.

Table 1

Time requirements for heating and cooling the extruder nozzle.

	200–210 (Δ 10°C)	200–300 (Δ 100°C)
heating	15 s (SD: 1.5)	104 s (SD: 3)
cooling	9.3 s (SD: 0.5)	47 s (SD: 3)

4.2.5. Purging materials

Purging the wood filament is necessary to prevent 3D printing with unwanted colors. If, for example, the system requires switching from a high temperature to a lower one, the filament present in the nozzle has already been heated (i.e., charred) and cannot be used to print the lighter shades. Therefore, purging the nozzle becomes essential to remove any residual material in the nozzle when the set temperature is lower than the current one (but unnecessary when the set temperature is higher or equal to the current one).

Purging in our system is implemented by extruding 15 mm of filament at two speeds, issuing the commands G1 E10 F500 and G1 E5 F1500 in sequence. This process was determined empirically by trial-and-error and ensures that no residual filaments remain clogged in the nozzle. The total purging time is 3 seconds.

4.3. Example applications

In this section, we showcase a variety of practical applications that exemplify the advantages of utilizing 3D printing with wood filament in multiple color shades across three distinct application domains.

4.3.1. Integrating esthetically pleasing elements in 3D objects

Colors enhance the appearance and increase the diversity of a 3D model without requiring modifications of the geometry. In contrast to previous approaches, our method accomplishes this using just a single filament. This is readily apparent in the examples of the *Pikachu*⁹ model (see Fig. 8a), where three distinct variations of the same model are visible. The leftmost *Pikachu* was printed with a single color shade (S_2 at 200°C, print time: 1 hrs 5 mins, filament consumed: 10 m), whereas the remaining models incorporated up to six discrete colors and three gradients applied to different surface patches (Fig. 8a — center *Pikachu*: 6 hrs 22 mins, 22.9 m, right *Pikachu*: 10 hrs 10 mins, 22.4 m). The tail and the right ear were printed using two vertical but opposed gradients, and the belt was printed with a single horizontal gradient.

Two other popular examples that allow direct comparisons with previous work [55] are the Stanford Bunny (Fig. 9c), which was printed with four shades and three gradients (S_1, S_3, S_5 , and S_{14}), and a safety cone (Fig. 8b, single color — 39 mins, 3.8 m; dual color — 3hrs 57 mins, 4.1 m), which was printed with two shades (S_4 and S_{16}). In addition to applying colors to specified surface regions, our system can also apply visual textures to cover a larger portion of the object surface, resulting in

⁸ <https://www.reprapfirmware.org>

⁹ <https://www.thingiverse.com/thing:376601>

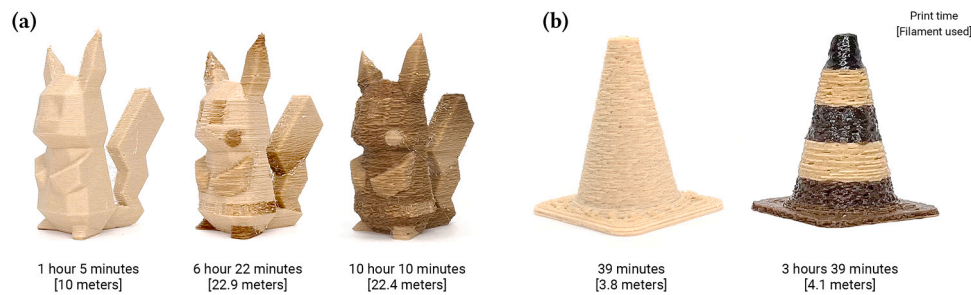


Fig. 8. a) Three Pikachu prints: the one on the left was printed in a single color shade—the default wood color of the filament. The other two (center, right) were printed using discrete patches and linear gradients of shades, resulting in visual variations without added geometries. b) Attempts to print two safety cones: the left one, printed in the default wood shade, fails to show the demarcations typical of safety cones, while the other one uses shades to create the distinguished look of safety cones.



Fig. 9. a) A wood log with bark details and different sized growth rings. b) Section view of the log revealing a natural transition between end grain and face grain textures. c) Stanford Bunny printed with 4 shades and 3 gradients.

more granular pixel-like control. For example, Fig. 7e shows a curved picture frame displaying the image of a zebra (1024 × 768) which was mapped to match the model's surface. Finally, Fig. 9a shows a wooden log split in two to demonstrate how the natural wood grain textures can be used to visually enrich the surface details of a 3D model that represents actual wood.

4.3.2. Embedding visual information in 3D objects

Using highly contrasting color shades also allows the embedding of visual information such as text and visual markings directly in the printed objects. Fig. 10a, for example, shows the text 'Pikachu' and a logo printed using multiple shades on the side of the character podium. Using high-contrast shades avoids modifications of the geometry (e.g., embossing or engraving) to make the text prominent.

Another usage of color shades is providing visual guidance on how to assemble or use a printed object. As an example, consider Fig. 10b, which showcases a pair of herringbone gears designed for a mirrored assembly, ensuring proper engagement of their teeth. Printing each side of the gears in distinct shades (W_1 and W_{16}) allows users to instantly and intuitively recognize the correct orientation.

For some applications, visually distinctive features with reduced tensile strength are desired. Fig. 10c depicts a modular cable manager with seven modules, each designed to be snapped off as needed. The modules are printed with the brightest shade (S_1 at 195°C), while the snap-off segments connecting the modules are printed with the darkest (S_{16} at 300°C). This high visual (and temperature) contrast serves the dual purposes of clearly demarcating the snap-off regions and also promotes a thermal degradation of the wood particles [22], creating predictable breaking points.

4.3.3. Embedding markers in 3D objects

Utilizing the pronounced visual contrast between light and dark color gradients (expressed as [51] $C_1 - 16 = \frac{S_{16} - S_1}{S_{16} + S_1} = 0.49$, $\Delta E = 44.8$), our approach proves to be well-suited for enhancing objects with digital markers. To illustrate, Fig. 11a showcases a wooden toy car body devoid of wheels, but with an augmented reality (AR) marker at its end. By employing a smartphone equipped with AR tracking software (i.e.,

Adobe Aero¹⁰), users can experience a seamless overlay of a complete digital rendering of the car atop the physical model. In another application (as depicted in Fig. 11c), we present a vase with a circular profile, deliberately crafted in a manner that allows the colors of distinct horizontal layers to be interpreted as a barcode (code-128¹¹), thereby facilitating the identification of its source model.

While it has been established by previous researchers that embedding AR markers [14] and barcodes [40] within 3D objects is feasible, our examples demonstrate that our technique accomplishes this with a distinctive advantage: only a single filament and extruder nozzle are necessitated in our approach. The print details for all the applications above are available in Table 2.

5. Discussion

In this section, we identify opportunities for further development and integrations with previous work. We also acknowledge limitations of our current approach.

5.1. Integrating pyrography craft with printing

3D printed pyrography allows applying different shades onto 3D objects by dynamically controlling the nozzle temperature. This approach can be further expanded by combining a more conventional pyrography approach [46] where a wood filament is heated after being printed through a soldering iron [46] or a heat gun [34]. This hybrid approach may have limitations because of its imprecise temperature control. However, it enables to carving of various patterns and textures into 3D printed objects [59]. It could also be a possible future solution for smoothing out the 3D printed wood filament through heat treating or manual polishing with a heated iron.

¹⁰ <https://www.adobe.com/products/aero.html>

¹¹ Barcode developed by Computer Identics Corporation (U.S.A.) in 1981. It can represent all 128 ASCII code characters

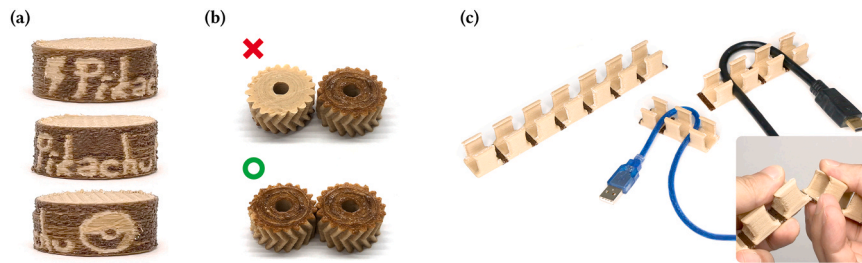


Fig. 10. a) Pikachu logo printed on the vertical surface of a puck-like podium. b) Herringbone gears in the incorrect and in the correct orientations. c) Modular snap-off cable manager with snapping points demarked by a high-contrast shade printed at a higher temperature.



Fig. 11. a) Body portion of a toy car with an AR marker printed on the front. b) AR overlay of the front nose and of a textured wheel using Adobe Aero app. c) A flower vase with a 1D barcode incorporated as a functional esthetic element.

5.2. Alternative materials for dynamic temperature control

Variable nozzle temperature during 3D printing can also affect non-wood-based materials, such as thermochromic [7] and varioShore [57] TPU filaments. When heated above its color transition temperature, thermochromic filament has color-changing properties, which can be engineered to have various thresholds [34]. While this color-changing effect is reversible, it is permanently deactivated when overheated (e.g., above 315°C [41]) as demonstrated previously with a laser cutter [58]. With our system we could selectively deactivate the filament’s color-changing capabilities.

Alternatively, varioShore filament [57] changes its mechanical

Table 2
Print statistics for each application.

Applications/ Print Details	Pikachu (Fig. 8a)	Safety cone (Fig. 8b)	“hi” (Fig. 7d)	Zebra (Fig. 7e)	Wood log (Fig. 9a)	Stanford bunny (Fig. 9b)	Podium (Fig. 10a)	Paired gears (Fig. 10b)	Cable manager (Fig. 10c)	Toy car (Fig. 11a)	Vase (Fig. 11c)
Multi color print time (hr:min)	6:22	3:57	2:49	11:05	4:28	4:00	2:48	2:03	2:13	5:33	18:44
Multi color Filament usage (m)	22.9	4.1	13.2	30.9	11.2	15.2	10.2	4.2	22.8	22.9	32.1
N. of shades/ gradients	6 (3)	2	4	5	3	4 (3)	3	2	2	3	2
Volume (cm ³)	289.3	80	25	201.9	61.5	134.8	50.2	22.5	107.2	280.2	663.8
Single color print time (hr:min)	1:05	0:30	0:35	1:13	0:29	0:42	0:25	0:20	1:07	1:17	2:25
Single color filament usage (m)	10	3.8	5.6	14.8	6.1	6.3	5.5	3.3	6.1	15.9	24

flexibility based on printed temperature. With this material, our system can also be extended to 3D print geometries with differently-flexible parts from a single filament [26,30].

5.3. Opportunities for pyrography beyond color shades

Pyrography with dynamic temperature control extends possibilities beyond mere visual effects. The maximum temperature for our extruder (E3D direct drive Hemera with a volcanic nozzle [16]) is capped at 300°C, however, using a higher-temperature nozzle (e.g., > 500°C [3,66]) could carbonize the wood particles in the filament [28]. However, high extrusion temperature may result in degradation of PLA, which degradation temperature is around 330°C [37]. Consequently, the carbonization of wood filament during extrusion requires the use of materials that combine wood particles with polymers capable of withstanding high temperatures, such as Polyamide Bioblends (i.e., bio-based nylons). These materials are known for their higher degradation temperatures (around 490°C [6]), making them suitable for such processes.

Wood filaments have also been employed for shape-changing objects in response to moisture [8,31]. Dynamic control over the printing temperature could possibly allow selective configurations of different parts of the geometry for higher water absorption when submerged [31]. Another possible objective for using 3D printing with dynamically changing temperatures is to control the mechanical properties of printed objects. For example, wood filament printed at high temperatures (> 230°C) exhibits reduced tensile strength [22] compared to filament printed below 230°C. This suggests possible research directions, such as the exploration of 3D-printed shock-absorbing objects (e.g., helmets and protectors) designed with predictable breaking points as exemplified in Fig. 10c.

5.4. Mechanical properties of wood filament printed across temperature

While the mechanical properties such as tensile strength (MPa),

modulus tensile strength (GPa), and brittleness are beyond the scope of this paper, we have observed that 3D printed structures weaken due to thermal degradation of the wood filament from high printing temperatures. Prior works [37,56] have experimented with the thermal degradation of wood filament with various wood particle ratios from 0% to 40% at temperatures ranging from 200°C to 600°C. It has been observed that both pure PLA and wood PLA decompose within the temperature range between 270°C to 350°C, with the highest rate of decomposition observed at 330°C [56]. The mass of both wood PLA and pure PLA can decrease up to 90% at 600°C [37]. Wood filaments are less thermally stable than pure PLA due to lower degradation temperature, and ash content increases with increased wood particle ratio [37]. From these study results, we hypothesize that the thermal degradation of wood filament, attributed to the shortening of polymer chains, likely contributes to a reduction in the filament's tensile strength and increased brittleness. To minimize the structural damage caused by thermal degradation of the filament when printed at high temperatures, we printed the inner structures (i.e., inner walls and infills) with the manufacturer's recommended temperature (195°C) [10] regardless of the color that is assigned to the outer surface.

5.5. Limitations for printing and slicing

The main limitations of this work pertains to the control of the nozzle temperature. For each color transition, the nozzle must heat up or cool down to reach the new target temperature. As a result, the printing time increases linearly with the number of color changes along the printing path. The time required for 3D printing increases with the addition of colors to the design. For example, a one-color safety cone (seen in Fig. 8b) is printed in 39 minutes using 3.8 m of filament, whereas a two-color version of the cone takes much longer: 3 hours and 57 minutes, with a filament usage of 4.1 m. This time discrepancy is amplified with the introduction of additional color shades. A single-color Pikachu (Fig. 8a — left) requires 1 hour and 5 minutes to print, consuming 10 m of filament. However, a Pikachu model featuring six shades and three gradient patterns significantly extends the printing time, taking either 6 hours and 22 minutes (Fig. 8a, middle) or as much as 10 hours and 10 minutes (Fig. 8a, right), depending on the color shades. Empirically, we observed that, at room temperature (26°C), cooling the nozzle was generally faster than heating it— by a factor of 1.5–2.2x depending on target temperature difference, which lets us marginally improve printing time by printing shades from light to dark. Future work will need to investigate methods for speeding up heating or cooling the nozzle, or software to optimize the color-change order.

Another limitation is the range of temperature that our nozzle can achieve (i.e., 300°C is our maximum supported temperature). The immediate consequence of this threshold is that, with the current setup, the maximum number of shade is limited to 16. On top of that, nozzle clogging is more likely to happen for wood fiber composite filaments. We have observed this limitation from our early explorations when we experimented with gradually changing the temperature from 195°C to 300°C while simultaneously extruding. This approach was not considered nor discussed in the paper because we immediately realized that it caused wood particle clustering and clogging (images of this exploration are included in the Appendix Figure A.3). This investigation led to our system implementing gradients by segmenting a path in discrete chunks with fixed temperatures, with the smallest path being 5 mm. Future work aiming to increase the maximum temperature threshold or supporting continuous gradients will need to carefully consider a suitable option for high-temperature nozzles.

This paper acknowledges certain limitations in the universal application of color on wood filaments. These include the number of discrete colors achievable and the fact that the specified temperature for color

change can vary. Additionally, the type of wood fiber used can influence the resulting color (e.g. pine-PLA [21] has a darker color than beech-fill filament [32]). Despite these limitations, this paper presents a detailed methodology for identifying shades of color in any wood filament used in 3D printing. To illustrate this, we conducted an identical process using a different wood filament (Lay Filaments' LayWoo-D3, which contains 40% recycled wood and 60% binding polymer). In this case, we observed 20 discrete colors, each with a JND being 1, and 13 colors each JND greater than 2.3. The full euclidean distance table, CIELAB color space and plotted RGB values are available in the Appendix Figure A.2.

Finally, we acknowledge the limitations of our custom G-code slicer. The slicer does not support conventional slicing features such as brim, raft, various infill patterns, bridging, and printing path optimization. We recognize these implementation issues, while also suggesting that, as in prior work about G-code generators [11,49,52], its capabilities are sufficient for our exemplary applications.

6. Conclusion

In conclusion, our paper presents *3D printed pyrography*, a simple yet novel technique that dynamically changes the printer's nozzle temperature to char wood-based filament while 3D printing. The wood filament exploration have identified that the wood filament can render distinguishable color shades ($\Delta E \geq 1$) with a temperature difference of 5°C. Among all 22 samples (minimum: 195°C, maximum: 300°C, increment: 5°C), we demonstrate printing 16 perceivably different shades of wood colors ($JND \geq 2.3$) from a single filament and extruder, without requiring hardware modification or special calibration. Our software system allows users to apply these 16 shades as discrete patches, 4 types of gradients, or mapped images as textures on 3D surfaces; the system automatically generates G-code for printing paths and for dynamically adjusting the nozzle temperature to achieve desired surface colors. Finally, to showcase the capabilities of 3D printed pyrography, we printed 11 applications showing how multiple shades can enhance or alter the visual esthetics of different 3D artifacts (e.g., Pikachu), display visual information about their usage (e.g., gears, cable manager), or embed digital markers (e.g., AR tracker) for tagging.

Author statement

Kongpyung (Justin) Moon - Conceptualization, Methodology, Software, Investigation, Writing – Original Draft, Writing – Review & Editing. **Jaeseong Yi** – Visualization, Methodology, Writing – Review. **Valkyrie Savage** - Methodology, Investigation, Writing – Review & Editing. **Andrea Bianchi** - Resources, Methodology, Formal analysis, Writing – Review & Editing, Supervision.

Declaration of Competing Interest

The authors declare that they have no known competing financial interests or personal relationships that could have appeared to influence the work reported in this paper

Data availability

Data will be made available on request.

Acknowledgments

This work was supported by the National Research Foundation of Korea (NRF) grant funded by the Korea government (MSIT) (No. 2018R1A5A7025409).

APPENDIX

Temperature	195°C	200°C	205°C	210°C	215°C	220°C	225°C	230°C	235°C	240°C	245°C	250°C	255°C	260°C	265°C	270°C	275°C	280°C	285°C	290°C	295°C	300°C
195°C	0.00	1.07	2.35	4.81	4.81	5.93	6.34	9.72	13.80	16.70	19.50	21.70	23.30	26.40	27.80	31.80	34.90	37.00	39.30	41.80	42.60	44.80
200°C		0.00	2.20	4.54	4.75	6.00	6.56	9.84	13.90	16.70	19.40	21.60	23.10	26.10	27.60	31.50	34.50	36.60	38.90	41.30	42.10	44.30
205°C			0.00	2.56	2.56	3.85	4.45	7.71	11.70	14.60	17.30	19.50	21.00	24.10	25.50	29.50	32.60	34.70	37.00	39.50	40.20	42.50
210°C				0.00	1.41	2.15	3.10	5.69	9.51	12.20	14.90	17.10	18.60	21.60	23.10	27.00	30.10	32.20	34.50	37.00	37.80	40.10
215°C					0.00	1.62	2.37	5.33	9.30	12.10	14.80	17.00	18.50	21.60	23.10	27.10	30.20	32.40	34.80	37.30	38.10	40.30
220°C						0.00	1.00	3.85	7.93	10.80	13.60	15.90	17.40	20.60	22.00	26.20	29.30	31.50	33.90	36.50	37.40	39.70
225°C							0.00	3.44	7.60	10.60	13.40	15.70	17.20	20.60	22.00	26.20	29.40	31.60	34.10	36.70	37.60	39.90
230°C								0.00	4.17	7.20	10.10	12.40	13.90	17.40	18.70	23.00	26.20	28.60	31.00	33.80	34.70	37.10
235°C									0.00	3.14	5.97	8.30	9.85	13.50	14.70	19.20	22.40	24.80	27.40	30.20	31.10	33.60
240°C										0.00	2.92	5.20	6.74	10.40	11.60	16.10	19.30	21.80	24.40	27.20	28.20	30.70
245°C											0.00	2.35	3.92	7.71	8.74	13.30	16.60	19.10	21.70	24.50	25.60	28.10
250°C												0.00	1.57	5.48	6.43	11.10	14.30	16.90	19.50	22.40	23.40	26.00
255°C													0.00	4.06	4.91	9.56	12.80	15.50	18.00	21.00	22.00	24.60
260°C														0.00	1.84	5.67	8.91	11.50	14.00	16.90	18.00	20.50
265°C															0.00	4.75	8.03	10.70	13.20	16.30	17.40	20.00
270°C																0.00	3.29	6.00	8.52	11.50	12.70	15.30
275°C																	0.00	2.97	5.35	8.39	9.57	12.20
280°C																		0.00	2.56	5.58	6.87	9.77
285°C																			0.00	3.09	4.45	7.43
290°C																				0.00	1.62	4.78
295°C																					0.00	3.25
300°C																						0.00

Fig. A.1. Table of Euclidean distances between all 22 samples (Colorfabb) that are printed between 195°C and 300°C, with 5°C increment.

(a)

Temperature	195°C	200°C	205°C	210°C	215°C	220°C	225°C	230°C	235°C	240°C	245°C	250°C	255°C	260°C	265°C	270°C	275°C	280°C	285°C	290°C	295°C	300°C
195°C	0.00	5.33	7.44	8.33	9.97	10.83	13.73	15.26	16.84	18.45	19.55	18.38	20.15	20.77	21.92	23.03	23.49	23.61	24.21	24.60	26.31	27.26
200°C		0.00	3.25	3.94	5.49	6.24	9.53	10.95	12.90	14.18	15.41	13.94	15.98	16.57	17.84	19.06	19.17	19.60	20.18	20.56	22.48	23.10
205°C			0.00	1.07	2.56	3.40	6.49	7.98	9.82	11.22	12.43	11.02	12.98	13.56	14.78	15.98	16.24	16.57	17.13	17.48	19.35	20.08
210°C				0.00	1.96	2.56	5.62	7.08	8.96	10.32	11.52	10.17	12.10	12.69	13.95	15.14	15.34	15.70	16.27	16.67	18.56	19.23
215°C					0.00	1.07	4.31	5.70	7.72	8.92	10.22	8.57	10.72	11.25	12.46	13.73	13.90	14.34	14.86	15.14	17.11	17.71
220°C						0.00	3.44	4.78	6.88	8.01	9.31	7.71	9.82	10.37	11.64	12.90	12.98	13.47	14.00	14.34	16.32	16.87
225°C							0.00	1.54	3.44	4.74	5.95	4.75	6.49	7.08	8.33	9.53	9.77	10.09	10.65	11.06	12.97	13.62
230°C								0.00	2.37	3.25	4.53	3.29	5.05	5.62	6.94	8.16	8.27	8.89	9.24	9.67	11.64	12.17
235°C									0.00	2.11	2.80	3.09	3.40	4.06	5.21	6.24	6.79	6.78	7.39	7.93	9.67	10.50
240°C										0.00	1.47	1.62	1.84	2.42	3.85	5.05	5.04	5.52	6.05	6.57	8.57	8.97
245°C											0.00	2.86	0.78	1.57	2.92	3.85	4.06	4.22	4.84	5.57	7.39	7.93
250°C												0.00	2.86	3.06	4.31	5.70	5.46	6.29	6.67	6.87	9.06	9.24
255°C													0.00	0.78	2.20	3.25	3.40	3.68	4.22	4.86	6.78	7.24
260°C														0.00	1.54	2.73	2.80	3.23	3.68	4.18	6.21	6.57
265°C															0.00	1.47	2.37	2.27	2.53	2.75	4.78	5.35
270°C																0.00	2.27	1.00	1.27	1.96	3.54	4.40
275°C																	0.00	2.04	2.04	2.73	4.64	4.18
280°C																		0.00	0.78	2.20	3.40	4.05
285°C																			0.00	1.54	2.80	3.29
290°C																				0.00	2.37	2.80
295°C																					0.00	2.53
300°C																						0.00

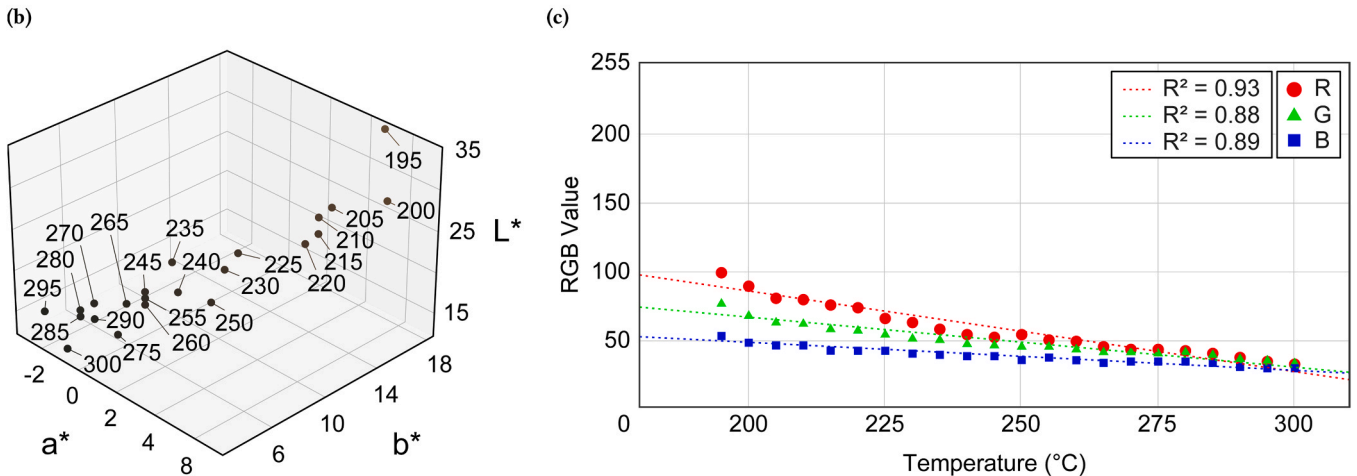


Fig. A.2. a) Table of Euclidean distances between all 22 samples (Laywood filament) that are printed between 195°C and 300°C, with 5°C increment. b) CIELAB plot. c) Relationship between printing temperature and RGB values.



Fig. A.3. Gradient exploration by extruding wood filament for 1500 mm with variable printing speed and extrusion rate. The nozzle temperature is initially set to 195°C and heats up to 300°C while extruding the material.

References

- [1] Danielle Albers Szafrir, Maureen Stone, and Michael Gleicher. 2014. Adapting Color Difference for Design. *Color and Imaging Conference* 2014.
- [2] Byoungkwon An, Ye Tao, Jianzhe Gu, Tingyu Cheng, Xiang 'Anthony' Chen, Xiaoxiao Zhang, Wei Zhao, Youngwook Do, Shigeo Takahashi, Hsiang-Yun Wu, Teng Zhang, Lining Yao, Thermorph: Democratizing 4D Printing of Self-Folding Materials and Interfaces. *Proceedings of the 2018 CHI Conference on Human Factors in Computing Systems* (Montreal QC, Canada) (CHI '18), Association for Computing Machinery, New York, NY, USA, 2018, pp. 1–12, <https://doi.org/10.1145/3173574.3173834>.
- [3] M.R. Assis, L. Brancheriau, A. Napoli, P.F. Trugilho, Factors affecting the mechanics of carbonized wood: literature review, *Wood Sci. Technol.* 50 3 (01 May 2016) (2016) 519–536, <https://doi.org/10.1007/s00226-016-0812-6>.
- [4] Zechun Ren Hongjie Bi, Min Xu Rui Guo, Yongming Song, Fabrication of flexible wood floor/thermoplastic polyurethane elastomer composites using fused deposition molding, *Ind. Crops Prod.* 122 (Oct. 2018) (2018) 76–84, <https://doi.org/10.1016/j.indcrop.2018.05.059>.
- [5] Thomas A. Campbell, Olga S. Ivanova, 3D printing of multifunctional nanocomposites, *Nano Today* 8 2 (2013) (2013) 119–120, <https://doi.org/10.1016/j.nantod.2012.12.002>.
- [6] Félix Carrasco, Orlando Santana Pérez, Maria Lluïsa Maspocho, Kinetics of the thermal degradation of poly(lactic acid) and polyamide bioblends, *Polymers* 22 (Nov. 2021) (2021), 13.
- [7] CC3D. 2023. *3D Printer Filament, heat-sensitive ThermoChromic Filament Material.* (https://www.amazon.com/dp/B074T8TGL5?ref=ast_sto_dp&th=1&psc=1).
- [8] Tiffany Cheng, Yasaman Tahouni, Dylan Wood, Benjamin Stolz, Rolf Mühlhaupt, Achim Menges, Multifunctional Mesostuctures: Design and Material Programming for 4D-Printing. *Proceedings of the 5th Annual ACM Symposium on Computational Fabrication* (Virtual Event, USA) (SCF '20), Association for Computing Machinery, New York, NY, USA, 2020, <https://doi.org/10.1145/3424630.3425418>.
- [9] H. Chung, Comparison in glass transition and enthalpy relaxation between native and gelatinized rice starches, *Carbohydr. Polymers* 3 (may 2002) (2002) 287–298, [https://doi.org/10.1016/S0144-8617\(01\)00259-4](https://doi.org/10.1016/S0144-8617(01)00259-4).
- [10] colorFabb. 2023. *WOODFILL.* (<https://colorfabb.com/woodfill>).
- [11] UltiMaker Cura. 2023. *UltiMaker Cura.* (<https://ultimaker.com/software/ultimaker-cura/>).
- [12] Atanu Kumar Das, David A. Agar, Magnus Rudolfsson, Sylvia H. Larsson, A review on wood powders in 3D printing: processes, properties and potential applications, *J. Mater. Res. Technol.* 15 (2021) (2021) 241–255, <https://doi.org/10.1016/j.jmrt.2021.07.110>.
- [13] Milena Djukanović, Ardijan Mavrić, Jovana Jovanović, Milovan Roganović, Velibor Bošković, Design of 3D printing thermo-sensored medical gear in detecting COVID-19 symptoms, *Appl. Sci.* 11 (1) (2021) 2021, <https://doi.org/10.3390/app11010419>.
- [14] Mustafa Doga Dogan, Ahmad Taka, Michael Lu, Yunyi Zhu, Akshat Kumar, Aakar Gupta, Stefanie Mueller, InfraredTags: embedding invisible AR markers and barcodes using low-cost, infrared-based 3D printing and imaging tools. *Proceedings of the 2022 CHI Conference on Human Factors in Computing Systems* (New Orleans, LA, USA) (CHI '22), Association for Computing Machinery, New York, NY, USA, 2022, <https://doi.org/10.1145/3491102.3501951>.
- [15] Duet3D. 2023. *Duet3D Documentation.* (https://docs.duet3d.com/User_manual/Reference/Gcodes#m109-set-extruder-temperature-and-wait).
- [16] E3D. 2023. V6 Nozzles. (<https://e3d-online.com/products/v6-nozzles>).
- [17] Josef Valentin Ecker, Andreas Haider, Ivana Burzic, Axel Huber, Gerhard Eder, Sabine Hild, Mechanical properties and water absorption behaviour of PLA and PLA/wood composites prepared by 3D printing and injection moulding, *Rapid Prototyp. J.* 4 (may 2019) (2019) 672–678, <https://doi.org/10.1108/rpj-06-2018-0149>.
- [18] Flashforge. 2023. FlashForge Creator 3 Pro. (<https://www.flashforge.com/>).
- [19] formlabs. 2023. *How to Prime and Paint 3D Printed Parts.* (<https://formlabs.com/blog/how-to-prime-and-paint-3d-prints/>).
- [20] Barry Fox. 1996. *Battery giants ready for battle over patent.* <https://www.newscientist.com/article/mg14920213-600-battery-giants-ready-for-battle-over-patent/>.
- [21] Marie-Joo Le Guen, Stefan Hill, Dawn Smith, Beatrix Theobald, Evamaria Gaugler, Abdellatif Barakat, Claire Mayer-Laigle, Influence of Rice Husk and Wood Biomass Properties on the Manufacture of Filaments for Fused Deposition Modeling, *Front. Chem.* 7 (Oct. 2019) (2019), <https://doi.org/10.3389/fchem.2019.00735>.
- [22] Sofiane Guessasma, Sofiane Belhabib, Hedi Nouri, Microstructure and mechanical performance of 3D printed wood-PLA/PHA using fused deposition modelling: effect of printing temperature, *Polymers* 11 (2019) (2019) 11, <https://doi.org/10.3390/polym11111778>.
- [23] Ferdinand Heinmets Julian T. Heinmets U.S. Patent 4156365 A, May, 1979. Temperature indicator.
- [24] Klaudius Henke, Sebastian Tremel, Wood based bulk material in 3D printing processes for applications in construction, *Eur. J. Wood Wood Prod.* 1 (Dec. 2012) (2012) 139–141, <https://doi.org/10.1007/s00107-012-0658-z>.
- [25] Stefan Hermann. 2017. Multi tone 3D printing with any 3D printer! (<https://www.youtube.com/watch?v=iT4hMj-2TM>).
- [26] Stefan Hermann. 2021. Super Soft TPU by FOAMING! - colorFabb varioShore TPU. (<https://www.youtube.com/watch?v=PtYaaBtm3XQ>).
- [27] Mirjam Hintz. 2023. *Hand-Painting 3D Prints with Acrylics.* (<https://justpaint.org/hand-painting-3d-prints-with-acrylics/>).
- [28] Ayaka Ishii, Kunihiko Kato, Kaori Ikematsu, Yoshihiro Kawahara, Itiro Sio, Fabricating Wooden Circuit Boards by Laser Beam Machining. *Adjunct Proceedings of the 34th Annual ACM Symposium on User Interface Software and Technology* (Virtual Event, USA) (UIST '21 Adjunct), Association for Computing Machinery, New York, NY, USA, 2021, pp. 109–111. (<https://doi.org/10.1145/3474349.3480191>).
- [29] M. Jurek, R. Wagnerová, Laser beam calibration for wood surface colour treatment, *Eur. J. Wood Wood Prod.* 79 (01 Sep 2021) (2021) 1097–1107, <https://doi.org/10.1007/s00107-021-01704-3>.
- [30] Hiroki Kaimoto, Junichi Yamaoka, Satoshi Nakamaru, Yoshihiro Kawahara, Yasuaki Kakehi, ExpandFab: Fabricating Objects Expanding and Changing Shape with Heat. *Proceedings of the Fourteenth International Conference on Tangible, Embedded, and Embodied Interaction* (Sydney NSW, Australia) (TEI '20), Association for Computing Machinery, New York, NY, USA, 2020, pp. 153–164, <https://doi.org/10.1145/3374920.3374949>.
- [31] Doron Kam, Michael Layani, Sheer Barkai Minerbi, Donna Orbaum, Shir Abrahami BenHarush, Oded Shoseyov, Shlomo Magdassi, 2019, Additive manufacturing of 3D structures composed of wood materials 2019 (9 Adv. Mater. Technol., 1900158 <https://doi.org/10.1002/admt.201900158> arXiv:https://onlinelibrary.wiley.com/doi/pdf/10.1002/admt.201900158 4.
- [32] Mirko Kariz, Milan Sernek, Manja Kitek Kuzman, Use of wood powder and adhesive as a mixture for 3D printing, *Eur. J. Wood Wood Prod.* 74, 1 (Nov. 2015) (2015) 123–126, <https://doi.org/10.1007/s00107-015-0987-9>.

- [33] Mirko Kariz, Milan Sernek, Murčo Obućina, Manja Kitek Kuzman, Effect of wood content in FDM filament on properties of 3D printed parts, *Mater. Today Commun.* 14 (2018) (2018) 135–140, <https://doi.org/10.1016/j.mtcomm.2017.12.016>.
- [34] Donghyeon Ko, Yeeun Shin, Junbeom Shin, Jiwoo Hong, Woolhun Lee, ChromoFilament: designing a thermochromic filament for displaying malleable states. *Proceedings of the 2022 ACM Designing Interactive Systems Conference* (Virtual Event, Australia) (*DIS '22*), Association for Computing Machinery, New York, NY, USA, 2022, pp. 1540–1554, <https://doi.org/10.1145/3532106.3533479>.
- [35] Rasika L. Kudahettige-Nilsson, Henrik Ullsten, Gunnar Henriksson, 2019, Plastic composites made from glycerol, citric acid, and forest components. *Bio Resources* 13, 3 (2019), 6600–6612. <https://doi.org/10.15376/biores.13.3.6600-6612> Cited by: 12; All Open Access, Bronze Open Access, Green Open Access..
- [36] Tim Kuipers, Willemijn Elkhuizen, Jouke Verlinden, Eugeni Doubrovski, Hatching for 3D prints: line-based halftoning for dual extrusion fused deposition modeling, *Comput. Graph.* 74 (2018) (2018) 23–32, <https://doi.org/10.1016/j.cag.2018.04.006>.
- [37] Sun-Young Lee, In-Aeh Kang, Geum-Hyun Doh, Ho-Gyu Yoon, Byung-Dae Park, Qinglin Wu, Thermal and mechanical properties of wood flour/talc-filled polylactic acid composites: effect of filler content and coupling treatment, *J. Thermoplast. Compos. Mater.* 21 3 (may 2008) (2008) 209–223, <https://doi.org/10.1177/0892705708089473>.
- [38] Eammon Littler, Bo Zhu, Wojciech Jarosz, Automated Filament Inking for Multi-Color FFF 3D Printing. *Proceedings of the 35th Annual ACM Symposium on User Interface Software and Technology* (Bend, OR, USA) (*UIST '22*), Association for Computing Machinery, New York, NY, USA, 2022. Article 83, 13 pages. <https://doi.org/10.1145/3526113.3545654>.
- [39] M. Mahy, L. Van Eycken, A. Oosterlinck, 1994, Evaluation of UniformColor Spaces Developed after the Adoption of CIELAB and CIELUV. *Color Research & Application* 19, 2 (1994), 105–121. <https://doi.org/10.1111/j.1520-6378.1994.tb00070.x> arXiv:<https://onlinelibrary.wiley.com/doi/pdf/10.1111/j.1520-6378.1994.tb00070.x>.
- [40] Henrique Teles Maia, Dingzeyu Li, Yuan Yang, and Changxi Zheng. 2019. LayerCode: Optical Barcodes for 3D Printed Shapes. *ACM Trans. Graph.* 38, 4, Article 112 (jul 2019), 14 pages. <https://doi.org/10.1145/3306346.3322960>.
- [41] Odwa Mapazi, Philemon K. Matabola, Richard M. Moutloali, Catherine J. Ngila, A urea-modified polydiacetylene-based high temperature reversible thermochromic sensor: characterisation and evaluation of properties as a function of temperature, *Sens. Actuators B Chem.* 252 (2017) (2017) 671–679, <https://doi.org/10.1016/j.snb.2017.05.095>.
- [42] Kongpyung (Justin) Moon, Haeun Lee, Jeeun Kim, Andrea Bianchi, ShrinkCells: Localized and Sequential Shape-Changing Actuation of 3D-Printed Objects via Selective Heating. *Proceedings of the 35th Annual ACM Symposium on User Interface Software and Technology* (Bend, OR, USA) (*UIST '22*), Association for Computing Machinery, New York, NY, USA, 2022, <https://doi.org/10.1145/3526113.3545670>.
- [43] Mosaic. 2023. Palette 3Pro. (<https://www.mosaicmfg.com/products/palette-e-3-pro>).
- [44] A. El Moumen, M. Tarfaoui, K. Lafdi, Modelling of the temperature and residual stress fields during 3D printing of polymer composites, *Int. J. Adv. Manuf. Technol.* 104 (June 2019) (2019) 1661–1676, <https://doi.org/10.1007/s00170-019-03965-y>, 5–8.
- [45] Rudy Plarre, Andrea Zocca, Andrea Spitzer, Sigrid Benemann, Anna A. Gorbushina, Yuexuan Li, Anja Waske, Alexander Funk, Janka Wilbig, Jens Günster, Searching for biological feedstock material: 3D printing of wood particles from house borer and drywood termite frass, *PLoS ONE* 16 (Feb. 2021) (2021) e0246511, <https://doi.org/10.1371/journal.pone.0246511>, 16.
- [46] Stephen Poole. 1995. *The Complete Pyrography*. CAMBRIDGE University.
- [47] X.Y.Z. Printing. 2023. da Vinci Color 3D Printer. (<https://www.xyzprinting.com/en/product/da-vinci-color>).
- [48] Josef Prusa. 2023. Original Prusa 3D printers directly from Josef Prusa. (<https://www.prusa3d.com/>).
- [49] PrusaSlicer. 2023. PrusaSlicer 2.6.0. (https://www.prusa3d.com/page/prusaslicer_424/).
- [50] Sakati. [n. d.]. 3DPrintColorizer: Software; hardware to do multi color printing with sharpies. (<https://github.com/Sakati84/3DPrintColorizer>).
- [51] William Shurcliff, *Studies in optics*: A.A. Michelson, University of Chicago Press, 1927, republished in 1962 as Phoenix Science series no. 514 paperback, 176 pp, *J. Phys. Chem. Solids* 24 (1963) (1963) 498–499, [https://doi.org/10.1016/0022-3697\(63\)90212-9](https://doi.org/10.1016/0022-3697(63)90212-9), 3.
- [52] Simplify3D. 2023. *Simplify3D 3D Printing Software*. (<https://www.simplify3d.com/>).
- [53] Stratasys. 2023. (<https://www.stratasys.com/en/3d-printers/printer-catalog/polyjet/>).
- [54] Lingyun Sun, Yue Yang, Yu Chen, Jiayi Li, Danli Luo, Haolin Liu, Lining Yao, Ye Tao, Guanyun Wang, ShrinCage: 4D Printing Accessories That Self-Adapt. *Proceedings of the 2021 CHI Conference on Human Factors in Computing Systems* (Yokohama, Japan) (*CHI '21*), Association for Computing Machinery, New York, NY, USA, 2021, <https://doi.org/10.1145/3411764.3445220>.
- [55] Haruki Takahashi, Parinya Punpongsonan, Jeeun Kim, Programmable Filament: Printed Filaments for Multi-Material 3D Printing. *Proceedings of the 33rd Annual ACM Symposium on User Interface Software and Technology* (Virtual Event, USA) (*UIST '20*), Association for Computing Machinery, New York, NY, USA, 2020, pp. 1209–1221, <https://doi.org/10.1145/3379337.3415863>.
- [56] Yubo Tao, Honglei Wang, Zelong Li, Peng Li, Sheldon Q. Shi, Development and application of wood flour-filled polylactic acid composite filament for 3D printing, *Materials* 10 (2017) (2017), <https://doi.org/10.3390/ma10040339>, 4.
- [57] VARIOSHORE TPU 2023. *WOODFILL*. (<https://colorfabb.com/varioshore-tpu-natural>).
- [58] Yuto Umetsu, Parinya Punpongsonan, Takefumi Hiraki, InfiniteShader: color changeable 3D printed objects using bi-stable thermochromic materials. *SIGGRAPH Asia 2022 Posters* (Daegu, Republic of Korea) (*SA '22*), Association for Computing Machinery, New York, NY, USA, 2022, <https://doi.org/10.1145/3550082.3564209>.
- [59] Sue Walters, *Pyrography Workbook: a complete Guide to the Art of Woodburning*, Fox Chapel Publishing, 2019.
- [60] Guanyun Wang, Ye Tao, Ozguc Bertug Capunaman, Humphrey Yang, Lining Yao, A-Line: 4D Printing Morphing Linear Composite Structures. *Proceedings of the 2019 CHI Conference on Human Factors in Computing Systems* (Glasgow, Scotland UK) (*CHI '19*), Association for Computing Machinery, New York, NY, USA, 2019, pp. 1–12, <https://doi.org/10.1145/3290605.3300656>.
- [61] Guanyun Wang, Humphrey Yang, Zeyu Yan, Nurcan Gecer Ulu, Ye Tao, Jianzhe Gu, Levent Burak Kara, Lining Yao, 4DMesh: 4D Printing Morphing Non-Developable Mesh Surfaces. *Proceedings of the 31st Annual ACM Symposium on User Interface Software and Technology* (Berlin, Germany) (*UIST '18*), Association for Computing Machinery, New York, NY, USA, 2018, pp. 623–635, <https://doi.org/10.1145/3242587.3242625>.
- [62] Tonghao Wu, Tenghao Yin, Xiaocheng Hu, Guodong Nian, Shaoxing Qu, Wei Yang, 2020, A Thermochromic Hydrogel for Camouflage and Soft Display. *Advanced Optical Materials* 8, 9 (2020), 2000031. <https://doi.org/10.1002/adom.202000031> arXiv:<https://onlinelibrary.wiley.com/doi/pdf/10.1002/adom.202000031>.
- [63] Michael J. Waters, Jessica M. Walker, Christopher T. Nelson, Derk Joester, James M. Rondinelli, 2020, Exploiting Colorimetry for Fidelity in Data Visualization. *Chemistry of Materials* 32, 13 (2020), 5455–5460. <https://doi.org/10.1021/acs.chemmater.0c00933> arXiv:<https://doi.org/10.1021/acs.chemmater.0c00933>.
- [64] Jiani Zeng, Honghao Deng, Yunyi Zhu, Michael Wessely, Axel Kilian, Stefanie Mueller, Lenticular Objects: 3D Printed Objects with Lenticular Lens Surfaces That Can Change Their Appearance Depending on the Viewpoint. *The 34th Annual ACM Symposium on User Interface Software and Technology* (Virtual Event, USA) (*UIST '21*), Association for Computing Machinery, New York, NY, USA, 2021, pp. 1184–1196, <https://doi.org/10.1145/3472749.3474815>.
- [65] Yizhong Zhang, Chunji Yin, Changxi Zheng, Kun Zhou, 2015, Computational Hydrographic Printing. *ACM Transactions on Graphics* (Proceedings of SIGGRAPH 2015) 34, 4 (Aug. 2015). <http://www.cs.columbia.edu/cg/hydrographics>.
- [66] Jun Zou, Wei Fang, Xuan He, Hui Chen, Xin Du, Tingting Jiang, Jiangping Qin, Lei Zhao, Carbonization temperature dependence of hydrovoltaic conversion of natural wood, *J. Mater. Sci.* 56 (01 Oct 2021) (2021) 16387–16398, <https://doi.org/10.1007/s10853-021-06345-8>, 29.